other matter. A decay or interference theory of short-term memory would predict a large drop in accuracy with aural presentation of the sequences.

ACKNOWLEDGMENT

The author would like to express his appreciation to Mrs. Susan A. Speeth for her help in these studies.

REFERENCES

[1] M. L. Benson, F. L. Crutchfield, and H. F. Hopkins, "Applications of touch-tone calling," *Elec. Engrg.*, vol. 81, pp. 262–267, April 1962.
[2] R. Conrad, "Accuracy of recall using keyset and telephone dial, and the effect of a prefix digit," *J. Appl. Psych.*, vol. 42, pp. 285–288, 1958.
[3] R. L. Deininger, "Human factors engineering studies of the design and use of pushbutton telephone sets," *Bell Sys. Tech. J.*, vol. 39, pp. 995–1012, 1960.
[4] W. K. Earl and J. D. Goff, "Comparison of two data entry methods," *Perceptual and Motor Skills*, vol. 20, pp. 369–384, 1965.
[5] F. J. Minor and S. L. Revesman, "Evaluation of input devices for a data setting task," *J. Appl. Psych.*, vol. 46, pp. 332–336, 1962.
[6] G. Rothert, "Influence of dials and pushbutton sets on errors, including the time required for the transmission of numbers," *Teleteknik* (English ed.), vol. 7, pp. 59–66, October 1963.
[7] S. Siegel, *Nonparametric Statistics for the Behavioral Sciences*. New York: McGraw-Hill, 1956.
[8] D. M. Schuster, "A human factors evaluation of switch actuators for use in spacecraft," *IEEE Trans. Human Factors in Electronics*, vol. HFE-6, pp. 33–42, September 1965.
[9] E. A. Wade and E. Cohen, "Population stereotypes in the directions of motion of thumbwheel switches," *Human Factors*, vol. 4, pp. 397–399, December 1962.

A Review of Quasi-Linear Pilot Models

DUANE T. McRUER, FELLOW, IEEE, AND HENRY R. JEX

***Abstract*—During the past several years, an analytical theory of manual control of vehicles has been in development and has emerged as a useful engineering tool for the explanation of past test results and prediction of new phenomena. An essential feature of this theory is the use of quasi-linear analytical models for the human pilot wherein the models' form and parameters are adapted to the task variables involved in the particular pilot–vehicle situation.**

This paper summarizes the current state of these models, and includes background on the nature of the models; experimental data and equations of describing function models for compensatory, pursuit, periodic, and multiloop control situations; the effects of task variables on some of the model parameters; some data on "remnant"; and the relationship of handling qualities ratings to the model parameters.

I. INTRODUCTION

A. The Nature of Pilot Models

THE TERMS in which engineering models are expressed are determined by the behavior they are to describe, by the type of problem they are expected to solve, and by the available techniques with which they are to be applied. Because the motivation for mathematical models of pilot response characteristics has been to explain the behavior of pilot–vehicle control systems, the analytical descriptions desired are in control engineering terms. The purposes of the models are to summarize behavioral data, to provide a basis for rationalization and understanding of pilot control actions, and, most important of all, to be used in conjunction with vehicle dynamics in forming predictions or in explaining the behavior of pilot–vehicle systems. The control engineering models which satisfy these desires are, at best, representations of pilot's *behavior* rather than mechanistic analogs of the pilot's physiological structure. The models are valid to the extent that their behavioral properties resemble or duplicate those of the human. They gain in acceptability if certain features can also be identified structurally, although they cannot be rejected because of any failure to satisfy this test. For a detailed background on the various types of human operator models which have been developed, the surveys in references [1]–[6] and the bibliographies of references [7] and [8] are recommended.

The human pilot is a multimode, adaptive,[1] learning controller capable of exhibiting an enormous variety of behavior, which includes:

1) System Organization

a) *Mechanization of Feedback Loops:* The selection and use of particular output motions of the vehicle

Manuscript received October 31, 1967; revised May 19, 1967. The vast majority of the original work on which this review draws was sponsored by the Flight Control Div. of the Air Force Flight Dynamics Lab., USAF Research and Technology Div., and the NASA Ames Research Center.

The authors are with Systems Technology, Inc., Hawthorne, Calif.

[1] As used here, these terms refer to improvements in some measure of performance over that of a fixed-parameter system; an *adaptive* system changes the performance in a *new* environment, while a *learning* system changes the performance in successive encounters with the *same* environment [3].

(from all of those capable of being sensed) which are best suited to serve as feedbacks to satisfy the guidance and control needs.

b) *Coherence Detection:* The extraction of coherence in the presented stimuli, including the abstraction of patterns in predictable functions.

c) *Coherence Utilization:*

i) *Mechanization of feedback loops*–The set-up of an internal organization (equivalent to the construction of several signal-processing paths within the human) to make efficient use of any coherence in the presented stimuli.

ii) *Command pattern generation*–The generation of internal anticipatory commands which, when transmitted to the effectors, results in a system output which duplicates the actual predictable forcing function.

2) System Adjustment

The adoption and adjustment of transfer characteristics appropriate for control of the system as organized. This phase also has two aspects.

a) *Central Aspects:* Associated with the sensory and equalization functions.

b) *Peripheral Features:* The adaptive adjustments of the neuromuscular subsystem.

Existing techniques for modeling are incapable of mimicking this complex behavior in a single grand model. Consequently, to obtain useful results, we must narrow our view and replace generality with specialization. By far the most fruitful specialized situations thus far considered are those of a stationary nature, where the task variables are constant and the pilot response characteristics are, because of training, reasonably stationary and repeatable. By considering such special situations, each of the many modes of behavior can be studied individually, as can the long term results of adaptation and learning within a particular mode. However, the dynamics of mode-switching and short-term adaptation and/or learning in the pilot, or of time-varying behavior in the task variables, cannot be treated with this approach.

B. Quasi-Linearization

To the extent that the physical situation has time-stationary properties, an appropriate approach is to model the possibly nonlinear pilot–vehicle system by some kind of quasi-linear system. This is an equivalent system in which the relationships between pertinent measures of system input and output signals are linear in spite of the existence of nonlinear elements. The quasi-linear system concept originally evolved from the observation that a great many nonlinear systems have responses to specific inputs which appear similar to responses of equivalent linear systems to these same inputs. For a given input–nonlinear-system combination, the response of the nonlinear system can be divided into two parts—one component which corresponds to the response of an equivalent linear element driven by that input, and an additional quantity, called the "remnant," which represents the difference between the response of the actual and the equivalent linear element. Quasi-linear models of a nonlinear system, for the specific input of interest, are represented mathematically by a "describing function," which is the equivalent linear element, plus the remnant, both of which may be input-dependent.

The most common quasi-linear system in engineering usage is the sinusoidal-input describing function, which is of great value in stability studies of nonlinear servomechanisms[9]–[11] and in the study of sinusoidal oscillations of the pilot–vehicle system, such as pilot-induced oscillations. Here, the describing function, when acted upon by a sinusoidal input, yields the Fourier fundamental component of the actual nonsinusoidal output. The remnant, which must be added to the output fundamental to achieve equivalence with the output signal of the nonlinear system, is made up of all the higher harmonics resulting from the passage of the sinusoid through the nonlinearity. Describing functions can also be defined for other periodic forcing functions, such as square waves; for transient inputs, such as step functions;[12] or for random inputs of specified stochastic properties [11], [13], [14]. In the last case, the remnant is also described by a random process, linearly uncorrelated with the input, which has a power spectral density such that the outputs of both the quasi-linear and the actual system have equal power spectral densities.[11]

Random-input describing function plus remnant descriptions are by far the most important quasi-linear models of the pilot–vehicle system. Not only are random forcing functions representative of important classes of piloting tasks, but their unpredictability precludes the pilot's coherence detection efforts. Describing functions based on random-appearing and periodic inputs have been the basis for the vast majority of pilot–vehicle system analyses, and have also received the lion's share of experimental effort. This paper is devoted to a summary of the current status of this type of pilot model, and how its parameters are affected by the task variables.

C. Key Variables in the Pilot–Vehicle System

The pilot's characteristics as a controller depend on four kinds of variables (see Fig. 1). The first are the *task variables*, which comprise all the system inputs and control system elements external to the pilot and which enter directly and explicitly into the pilot's control task. Four of these—forcing function, display, manipulator, and controlled element dynamics—have a major effect on the pilot dynamics. The second type of variable affecting the pilot's operation is the *environment* external to the pilot. Environmental variables include such factors as ambient illumination, temperature, vibration, and G-loading (to the extent that this is superimposed on, rather than controlled by, the pilot). The third type of variable is *operator-centered.* This includes such things as training, fatigue, and motivation. Finally, for a given experimental series there are *procedural* variables, such

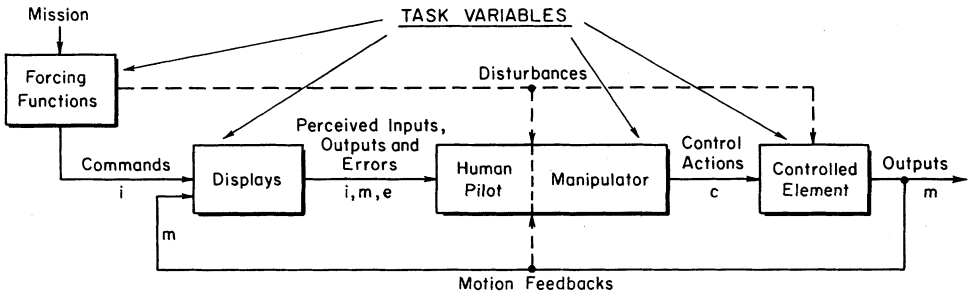

ENVIRONMENTAL VARIABLES:	OPERATOR-CENTERED VARIABLES:	PROCEDURAL VARIABLES:
In-Flight vs. Fixed-Base	Motivation	Instructions
Vibration	Stress	Practice
G-Level	Workload	Experimental Design
Temperature	Training	Order of Presentation
Atmospheric Conditions	Fatigue	Etc.
Etc.	Etc.	

Fig. 1. Variables affecting the pilot-vehicle system.

as instructions, practice, order of presentation, etc., which can be very important to the accuracy and generality of the experimentally based conclusions.

The impact of the operator-centered and procedural variables has been minimized, in the data reported herein, by using highly trained and motivated subjects drawn from a narrowly limited population for which high grade skill in piloting tasks is an essential feature; carefully tieing in results from one experimental series with those of others; and using balanced experimental designs to the extent feasible. For all of the models described here the environmental variables have been those corresponding to either fixed-base or straight-and-level flight conditions. Recently the effects of environmental characteristics on pilot describing functions have received attention elsewhere,[15]-[17] so these will not be considered herein.

With these introductory remarks, the subject has been specialized to quasi-linear describing function and remnant models as affected by task variables. Nevertheless, as will be seen, the scope of even this specialized area is considerable.

II. Pilot Describing Function Models

A. The Crossover Model

The most important class of situations for which pilot–vehicle models are useful are closed-loop compensatory tracking tasks in which the pilot acts on the displayed error e between a desired command input i and the comparable vehicle output motion m to produce a control action c. The power servo, vehicle, sensor, and display dynamics are all combined into the controlled element dynamics, having a transfer function $Y_c(s)$. The portion of the pilot's control action linearly correlated with the input is represented by the quasi-linear describing function $Y_p(j\omega)$, which also includes the effects of the manipulator "feel" characteristics.[2] The forcing function (command input or internal disturbance) must be subjectively random-appearing. It is idealized as a stationary random signal having a Gaussian amplitude distribution with rms level σ_i and a low-pass frequency characteristic with bandwidth ω_i. The goal is to follow commands and regulate against disturbances; in other words, to minimize error. Under these conditions the pilot becomes a serial element in the closed-loop system and, given sufficient practice, evolves a stable relationship between his control action and the particular set of displayed signals.

The human pilot has the capability of adjusting or equalizing his behavior so that the closed-loop characteristics fulfill the basic conditions required of any good feedback control system. These are to:

1) provide some desired command-response relationship;
2) suppress unwanted inputs and disturbances;
3) reduce the effects of variations and uncertainties in the components of the control loop;
4) provide adequate closed-loop stability margins.

In a compensatory control loop, these four functions are accomplished by making the amplitude ratio of the open-loop frequency response, $|Y_{OL}| = |Y_pY_c|$, very large over the frequency range of the input bandwidth and very small outside this range. Unfortunately, an extremely sharp change in amplitude ratio with frequency cannot generally be realized due to accompanying phase lags which destabilize the closed-loop system. Allowing for the stability requirements of positive gain margin and phase margin, the compromise between high gain over

[2] The pilot's describing function is written herein in terms of the frequency operator ($j\omega$) instead of the general Laplace variable ($s = \sigma + j\omega$) to emphasize that it is strictly valid only in the frequency domain (i.e., with continuous randomlike inputs) and should not be used, without appropriate modification, to compute the system response to a deterministic input such as a step.

the input bandwidth and low gain beyond the input bandwidth is embodied in a *Primary Rule of Thumb for Frequency Domain Synthesis* (adapted from McRuer and Graham.[18])

> "At frequencies just within and beyond the input bandwidth, seek or create (by equalization) a fair stretch of −20 dB/decade slope for the amplitude ratio and adjust the loop gain so as to put the unity-amplitude crossover frequency near the higher edge of this region, while maintaining adequate stability margins."

The region near crossover frequency, ω_c (i.e., where $|Y_{OL}| = 1.0$, or 0 dB) is of fundamental importance in the analysis of closed-loop piloting tasks for the following reasons.

1) For the system output to approximate the input (tracking errors to be small), ω_c must exceed ω_i.
2) The nature of Y_{OL} near ω_c determines the dominant closed-loop modes and response, e.g., the displayed error spectrum generally shows a peak near this frequency.
3) The system stability is determined by the open-loop gain and phase characteristics near this frequency.

A fairly comprehensive understanding of the effect of task variables on the pilot model and on the resulting closed-loop performance is available from a very extensive and recent set of data[19] together with earlier data summarized in the references.[20], [21] *The most significant result of these measurements is the degree to which all of the data—for controlled elements ranging from $Y_c = K_c$, through K_c/s, to K_c/s^2—approach the characteristics dictated by the Primary Rule of Thumb in the crossover region.* The pilot adopts sufficient lead or lag equalization so that the slope of $|Y_{OL}| = |Y_pY_c|$ lies very close to −20 dB/decade in the region of crossover frequencies. Besides the −90 deg phase shift associated with the −20 dB/decade amplitude ratio, there is an accumulation of additional lags due to transport delays and high frequency neuromuscular dynamics. All of these can be represented (near crossover frequencies) by an effective time delay τ_e. Consequently, a remarkably simple two-parameter "crossover model" can account for most of the significant open-loop data trends in the important crossover frequency region.

The *crossover model* is

$$Y_{OL}(j\omega) = Y_pY_c \doteq \frac{\omega_c e^{-j\omega\tau_e}}{j\omega}; \quad \text{near } \omega_c. \tag{1}$$

The crossover frequency ω_c is equivalent to the loop gain and accounts for the pilot's adaptive compensation for the controlled element gain. Both ω_c and τ_e are functions of the task variables. This simple crossover model is not a replacement for the complete verbal-analytical pilot model (which will be given later) but is a convenient approximation suitable for many pilot–vehicle engineering purposes. It is a better approximation of the amplitude ratio data than of the phase data. Furthermore, it usually leads to essentially correct closed-loop characteristics because the actual shape of the open-loop describing function far from the crossover region usually has little effect on the closed-loop dynamics.

To illustrate these basic and important points, typical measured pilot–vehicle describing functions for three types of controlled elements are shown in Fig. 2 (see McRuer *et al.*[19] for further details). Also shown are the controlled element transfer functions alone (dotted lines) and the fitted crossover model (solid lines) having the form of (1). The difference between the dotted lines and data points represents the pilot's equalization, which is a lag for $Y_c = K_c$, none for $Y_c = K_c/s$, and a lead for $Y_c = K_c/s^2$. The main point is that *all* cases end up being reasonably well fitted by the crossover model over a wide frequency range below and near crossover, with different parameters for different Y_c's.

These data are typical of other controlled elements having at most one pole in the crossover region and capable of being equalized to the crossover model form by a single lead or lag. The crossover model is even a fairly good fit to situations involving a mildly unstable controlled element which must be stabilized by the pilot's control action. However, when the degree of instability is severe, the pilot's behavior is constrained to a narrow range by vanishing stability margins which may preclude equalization to the −20 dB/decade criterion. Further data and discussion of this interesting facet is beyond the scope of this paper, but is covered in references [19], [22], [23]. Many aerospace vehicle systems can be approximated by one of these simpler controlled elements in the (final) crossover region. Some simple examples are given in Table I and a bibliography for more complex application examples is given in reference [7].

B. Form of Pilot Describing Function and Equalization Adjustment

The simplest pilot describing function form, which corresponds to the open-loop crossover model, is:

$$Y_p = K_p \frac{(T_L j\omega + 1)}{(T_I j\omega + 1)} e^{-j\omega\tau_e} \tag{2}$$

where

K_p = pilot static gain
T_L = lead time constant (relative rate-to-displacement sensitivity)
T_I = lag time constant
τ_e = effective time delay, including transport delays and high frequency neuromuscular lags.

The lead and lag equalization T_L and T_I are adjusted by the pilot to achieve the −20 dB/decade slope of the combined Y_pY_c response, as required by the crossover model, while the gain K_p is adjusted to put ω_c where required. It appears that the pilot attempts to choose a lead or lag value such that the sensitivity of the closed-loop low-frequency characteristics to variations in T_L

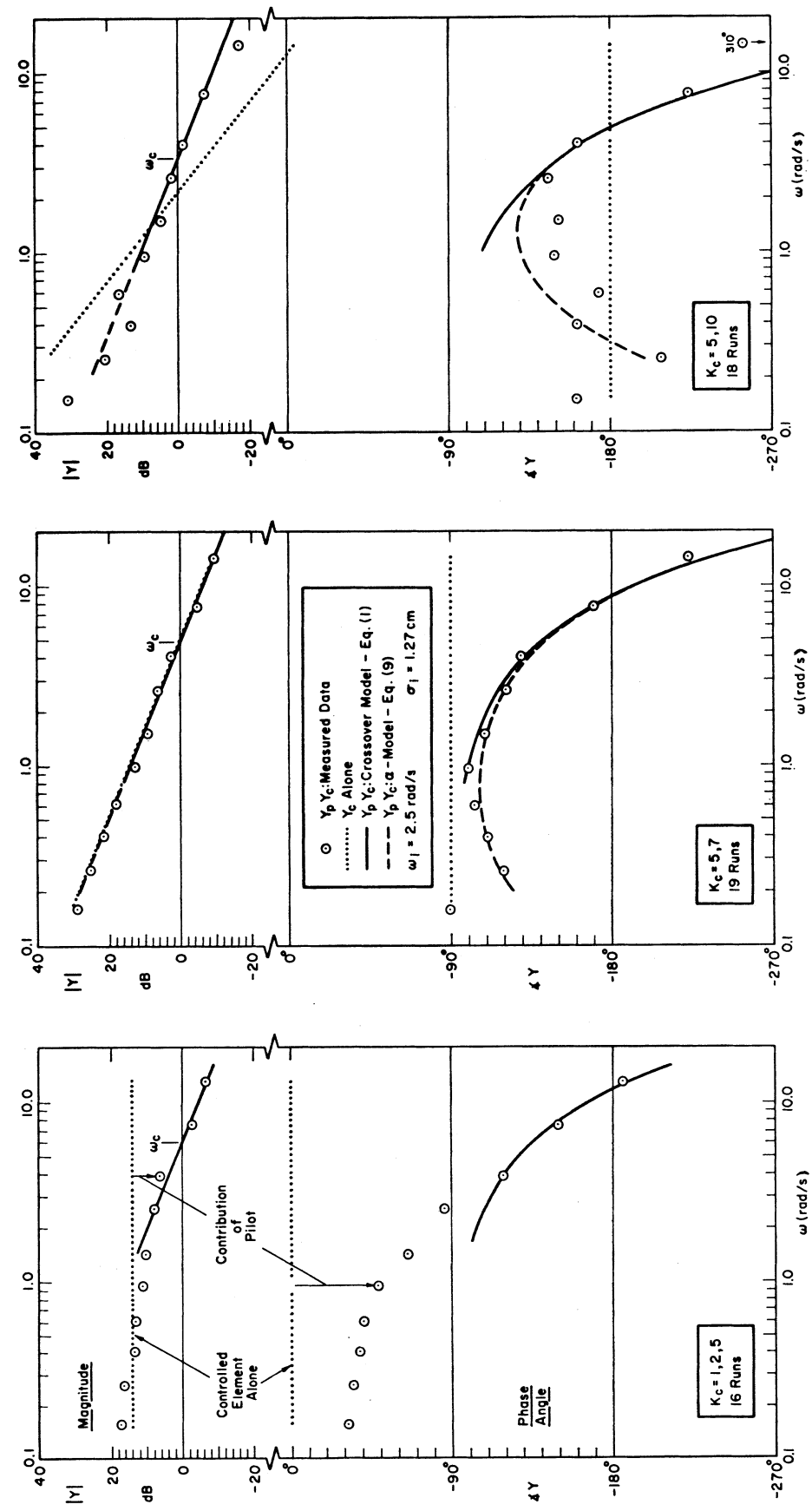

(a) $Y_c = K_c$ (b) $Y_c = K_c/s$ (c) $Y_c = K_c/s^2$

Fig. 2. Measured open-loop describing functions and comparisons with crossover models for $Y_c = K$, K/s, and K/s^2.

TABLE I
TYPICAL AIRCRAFT CONTROL TASKS AND RELATED SIMPLE CONTROLLED ELEMENT

Controlled Element	Related Vehicle Control Situations
$Y_c \doteq K_c$	Aircraft load factor control (at high speeds) by elevator
$Y_c \doteq \frac{K_c}{s}$	Aircraft pitch angle control by elevator Attitude control of vehicles with augmented damping Automobile heading control by steering wheel
$Y_c \doteq \frac{K_c}{s^2}$	Space vehicle attitude control by control jets Rocket booster control (at launch) by thrust deflection Aircraft heading control by ailerons
$Y_c \doteq \frac{K_c}{s(s + 1/T)}$	Aircraft roll angle control by ailerons V/STOL translation control (at hover) by thrust deflection
$Y_c \doteq \frac{K_c}{(s - 1/T)}$	Pitch angle control of a statically unstable aircraft by elevator
$Y_c \doteq \frac{1}{s(s - 1/T)}$	Unstable rocket booster control (at high dynamic pressure) by thrust deflection

or T_I is small, leaving the gain and effective time delay as his primary means for adjusting the closed-loop stability and dominant modes.

The resulting equalization adjustment rule in verbal form is as follows.

Rule 1—Equalization Selection and Adjustment: The particular equalization is selected from the general form $K_p(T_L j\omega + 1)/(T_I j\omega + 1)$ such that the following properties occur.

a) The system can be stabilized by proper selection of gain K_p preferably over a very broad range of K_p.
b) Over a wide frequency range, near the crossover region, the magnitude ratio $|Y_p Y_c|$ has approximately a —20 dB/decade slope.
c) $|Y_p Y_c| \gg 1$ is obtained at low frequencies to provide good low frequency closed-loop response to system commands and suppression of disturbances.

Examples of equalization selection and basic adjustment are provided in Table II for a variety of simple controlled elements based on data in McRuer *et al.*[19]

C. Adjustment of Crossover Frequency and Effective Time Delay

Once the basic form of equalization has been adopted by the pilot to stabilize the system, he then adjusts the system parameters so as to tend to minimize the tracking errors if he is so instructed.[19], [21], [24] Other criteria than minimum error can affect the adjustments, e.g., under extreme adaptation conditions (for instance, near the pilot's force or lead equalization limits), or with a cost criterion involving other quantities (such as "minimize the displayed sum of error squared and control deflection squared").[25], [26] As a practical matter, minimizing tracking errors is tantamount to minimizing the mean-square error because:

> Under fairly general conditions, a quasi-linear system adjusted to give minimum mean-square error for Gaussian inputs also minimizes a large number of other monotonic error criteria.[27]
> Experienced pilots, when told merely to "minimize the errors," exhibit performance and response measures which are indistinguishable from that when told to "minimize their mean-square-error tracking score" (Obermayer *et al.*,[28] Experiment V).

As a general statement, the second rule of adaptation is as follows.

Rule 2: Within the pilot's intrinsic limitations, and once the —20 dB/decade amplitude ratio slope has been achieved, the adjustments of crossover frequency and effective time delay are such as to minimize the mean-square error (for $\omega_i \ll \omega_c$).

This rule cannot be applied without a more complete definition of the "intrinsic limitations" and adjustments. Fortunately, the experiments in McRuer *et al.*[19] have shed empirical light on these, but the adjustments are difficult to describe in a neat, sequential manner.

In terms of the crossover model, the parameters at hand to minimize error are the crossover frequency and τ_e. In general, increasing gain (crossover frequency), or increasing the phase margin φ_M (through reduced τ_e), and thereby the damping of the closed-loop dominant modes, each tends to reduce the system errors. Were it not for the unavoidable human operator lags represented by τ_e, the pilot could increase his gain without limit once the open-loop amplitude ratio is equalized to the $|\omega_c/j\omega|$ form, because the corresponding phase lag would be only —90 deg out of the —180 deg allowed. However, τ_e reduces the phase margin and ultimately limits ω_c to less than 10 rad/s. For the crossover model, the dependence of φ_M on τ_e is given by

$$\varphi_M = \frac{\pi}{2} - \tau_e \omega_c \text{ (angles in radians)} \tag{3}$$

and the error/input ratio at ω_c is

$$\left|\frac{e}{i}\right|_{\omega_c} = \frac{1}{2 \sin (\varphi_M/2)} \doteq \frac{1}{\varphi_M(\text{rad})} \Bigg|_{\alpha_M \ll 1} . \tag{4}$$

Note that the $|e/i|$ ratio peak generally occurs at a higher frequency than ω_c while the error spectrum peak depends on both the ω_c and the $|e/i|$ spectrum shapes.

One of the most interesting findings in McRuer *et al.*[19] was that the crossover frequency is strongly dependent on the form of controlled element, but less dependent on input bandwidth (see Fig. 3). It was further found that ω_{c_0}, the value of neutrally stable crossover frequency for $\omega_i = 0$ (found by extrapolation) corresponds to the basic time delay τ_0, inferred by extrapolating τ_e versus ω_i to vanishingly low input bandwidths (Fig. 4). This basic "relaxed" level of τ_0 is the value of τ_e when no high-frequency lead is used to help cancel neuromuscular lags

TABLE II
PILOT EQUALIZATION ADJUSTMENT FOR VARIOUS CONTROLLED ELEMENTS

Controlled Element Approximate Transfer Function in Crossover Region $Y_c(s)$	Pilot's Equalizer Form	Pilot's Describing Function $Y_p(j\omega)$	Location of Equalization Break Frequency
K_c	Lag-lead	$\frac{K_p e^{-j\omega\tau_e}}{(T_I j\omega + 1)}$	$\frac{1}{T_I} \ll \omega_c$
$\frac{K_c}{s}$	High-frequency lead	$K_p e^{-j\omega\tau_e}$	—
$\frac{K_c}{s^2}$	Low-frequency lead	$K_p(T_L j\omega + 1)e^{-j\omega\tau_e}$	$\frac{1}{T_L} \ll \omega_c$
$\frac{K_c}{s(Ts + 1)}$	If $T > \tau_e$ use mid-frequency lead	$K_p(T_L j\omega + 1)e^{-j\omega\tau_e}$	$\frac{1}{T_L} \doteq \frac{1}{T}$
	If $T < \tau_e$ use high-frequency lead	$K_p e^{-j\omega\tau_e}$	—
$\frac{K_c}{\left(\frac{s}{\omega_n}\right)^2 + \frac{2\zeta}{\omega_n} s + 1}$	If low natural frequency ($\omega_n \ll 1/\tau_e$) use low-frequency lead	$K_p(T_L j\omega + 1)e^{-j\omega\tau_e}$	$\frac{1}{T_L} \ll \omega_c$
	If high natural frequency ($\omega_n > 1/\tau_e$) use lag-lead	$\frac{K_p e^{-j\omega\tau_e}}{(T_I j\omega + 1)}$	$\frac{1}{T_I} \ll \omega_c$

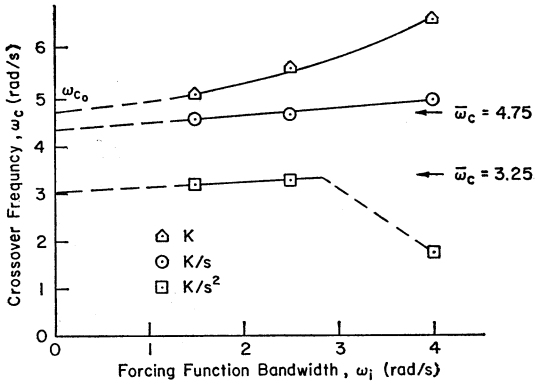

Fig. 3. Dependence of crossover frequency on type of controlled element and input bandwidth.

and the neuromuscular system is fairly relaxed and sluggish. Thus ω_{c_0} can be estimated by using τ_0 for τ_e and solving $Y_{OL}(j\omega) = -1$ for the gain and frequency at neutral stability. If a large stretch of -20 dB/decade amplitude exists, then ω_{c_0} can often be estimated by Rule 3.

Rule 3—Crossover Frequency:

$$\omega_{c_0} \doteq \frac{\pi}{2\tau_0}. \tag{5}$$

When Rule 3 is applied to more complex controlled elements, it is important that all time delays in the controlled element and display be included in τ_0. While ω_c increases slightly with ω_i, the average value $\bar{\omega}_c$ of the crossover frequency over all ω_i is only slightly larger than ω_{c_0}.

Once this crossover frequency is fixed, the operator's primary adjustment to an increase in forcing function bandwidth is to increase his closed-loop damping ratio

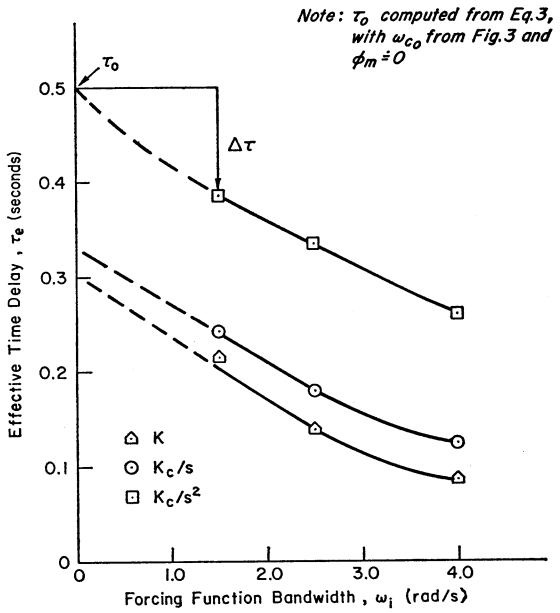

Fig. 4. Variation of effective time delay on type of controlled element and input bandwidth.

so that the closed-loop amplitude ratio peak resulting from the low phase margin does not contribute appreciably to the tracking errors. He does this by decreasing his effective time delay by tightening up on his neuromuscular loop (e.g., a tighter grip on the control stick), or by adding some high-frequency lead equalization (provided it is not required for the basic equalization as noted previously in Table II), or both.

However, as ω_i approaches ω_{c_0}, it can be shown (19) that retention of the crossover frequency near ω_{c_0} results in normalized errors greater than 1.0. Under these condi-

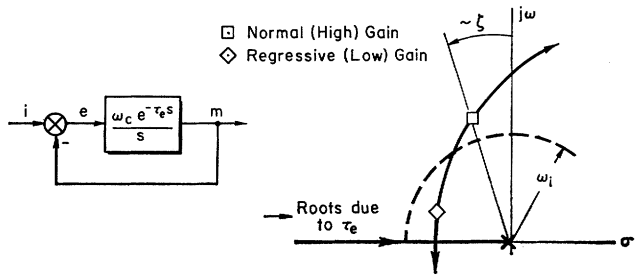

(a) Root locus

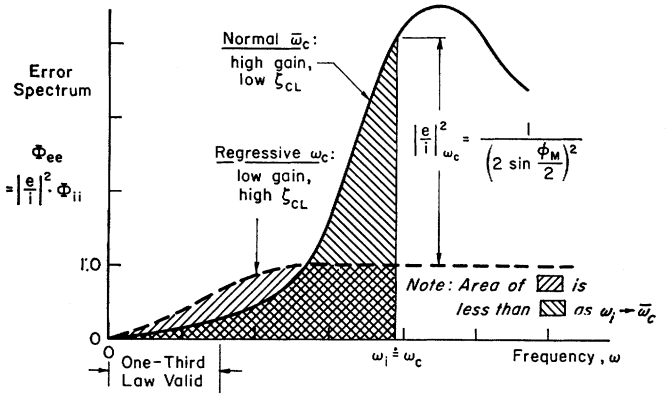

(b) Error spectra are to rectangular input spectrum

Fig. 5. Sketch of the factors causing crossover regression.

tions, the pilot "regresses" to a low gain technique (i.e., a lower ω_c) and simply ignores the high-frequency input components. This crossover regression phenomenon is illustrated in Fig. 5, where the areas under the curves are proportional to the mean-square error for a rectangular input spectrum of bandwidth ω_i. It can be seen that for wide-band inputs ($\omega_i \doteq \omega_c$) the resonant peak dominates the error, so a lower gain is beneficial. Crossover regression can be seen in the data of Fig. 3 for the K_c/s^2 case at $\omega_i = 4$.

The foregoing crossover frequency relationships are summarized in the "ω_c invariance properties" of Rule 4.

Rule 4:

a) ω_c—K_c independence: After initial adjustment, changes in controlled element gain, K_c, are offset by changes in pilot gain, K_p; i.e., system crossover frequency, ω_c, is invariant with K_c.
b) ω_c—ω_i independence: System crossover frequency depends only slightly on forcing function bandwidth for $\omega_i < 0.8\omega_c$.
c) ω_c regression: When ω_i nears or becomes greater than $0.8\omega_{c_0}$, the crossover frequency regresses to values much lower than ω_{c_0}.

Under favorable tracking conditions ($\omega_i \ll \omega_c$, relatively small remnant, etc.) a very simple approximation to the command tracking error can be found from the "one-third law" derived in McRuer and Krendel.[29]

TABLE III
VALUES OF ω_c, τ_0, AND $\Delta\tau$ VS. Y_c

Y_c in crossover region	$\bar{\omega}_c$ (rad/s)	τ_0 (seconds)	$\Delta\tau$ (seconds)
K_c	5 to 6	0.33	$0.070\ \omega_i$
K_c/s	4.3	0.36	$0.065\ \omega_i$
K_c/s^2	3.3	0.50	$0.065\ \omega_i$

Rule 5:

$$\frac{\overline{e_i^2}}{\overline{i^2}} \doteq \frac{1}{3}\left(\frac{\omega_i}{\omega_c}\right)^2. \tag{6}$$

This relationship is useful in the scaling of displays and inputs, and in assessing the performance potential of alternative pilot loop closures.

Effective time delay: The measured and cross-plotted data for τ_e from McRuer *et al.*[19] are shown in Fig. 4. It is apparent that τ_e decreases with ω_i, with a slope practically independent of the controlled element, while the basic level of τ_e depends primarily on the controlled element, independent of ω_i. Thus an empirical relationship for τ_e as a function of its dominant task variable, for relatively low input bandwidths, can be written as:

Rule 6:

$$\tau_e(Y_c, \omega_i) \doteq \tau_0(Y_c) - \Delta\tau(\omega_i). \tag{7}$$

Putting in the average slopes of $\Delta\tau/\Delta\omega_i$ from Fig. 4, and collecting all the quantities in tabular form, gives the relations tabulated in Table III.

Remember that these are average values for a number of skilled pilots in a particular fixed-base simulator, with a spring-loaded stick and single-axis cathode-ray-tube display. They are thus representative, but may not be exactly duplicated in a different setup.

D. Refinements to the Model

The simple crossover model for single-loop pilot-vehicle control is best suited to conventional stable controlled elements which have smooth amplitude and phase characteristics in the potential crossover region, for tasks where the input is at low frequencies, and where the remnant is relatively small. In other situations more accuracy is desired, as when the controlled element break frequencies are in the crossover region or in conditionally stable systems. More refined operator describing function models have been developed to handle these cases,[19] always balancing the need for improvement in accuracy against the inevitably increased complexity and number of parameters involved.

One such refinement is the "extended crossover model" or "α model." This is especially useful for conditionally stable systems (e.g., when a pilot is stabilizing an unstable controlled element). Such situations result in low

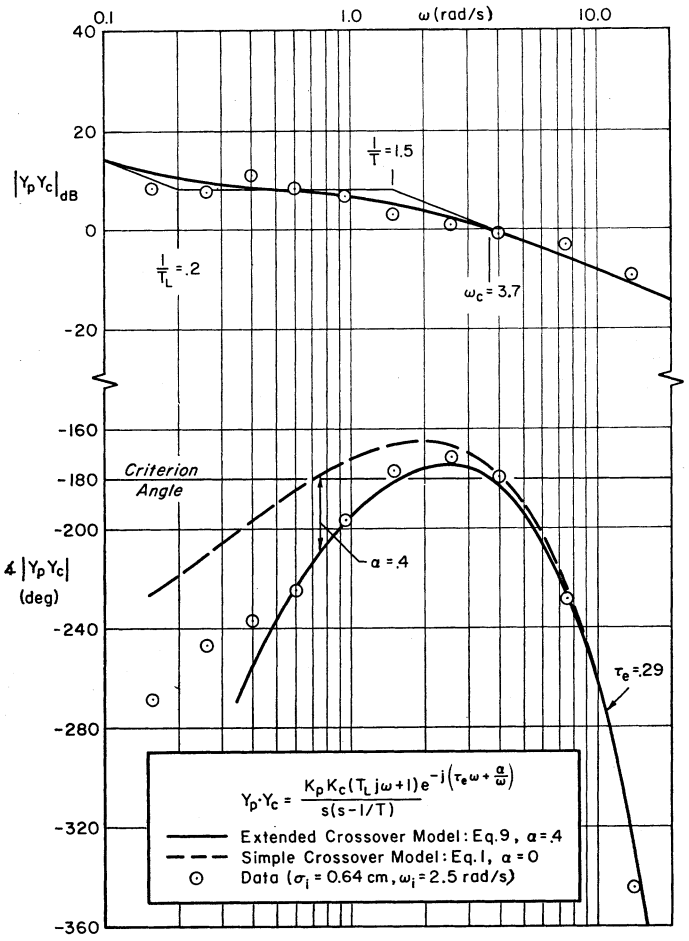

Fig. 6. Comparison of $\alpha = 0$ and $\alpha = 0.4$ extended crossover model fits with $Y_c = K_c/s$ $(s—1/T)$.

phase margins which limit the extent of the stable crossover region and require a fairly accurate phase representation at mid-band frequencies.

The primary purpose of the extended crossover model is to account for the low-frequency phase droop, which can be seen in Fig. 2. The mid-frequency influence of this phase lag contribution can significantly reduce the phase margins in cases where the vehicle is unstable or the operator's lead-equalizing ability is being severely strained. This phase droop is attributed to very-low-frequency dynamics with amplitude ratio breakpoints below the measurable bandwidth in most experiments. It is shown[19] that the net phase contribution at mid-frequencies can be approximated by

$$\Delta\varphi_{\text{mid}} \doteq \frac{\alpha}{\omega} \text{ (angles in radians).} \tag{8}$$

This "α effect" is summed with the effective time delay to form the pure phase lag contributions of the extended crossover model, or α model, and the pilot's describing function becomes

$$Y_p(j\omega)_{\alpha\ \text{model}} \doteq \frac{K_p e^{-j(\tau_e\omega + \alpha/\omega)}(T_L j\omega + 1)}{(T_I j\omega + 1)}. \tag{9}$$

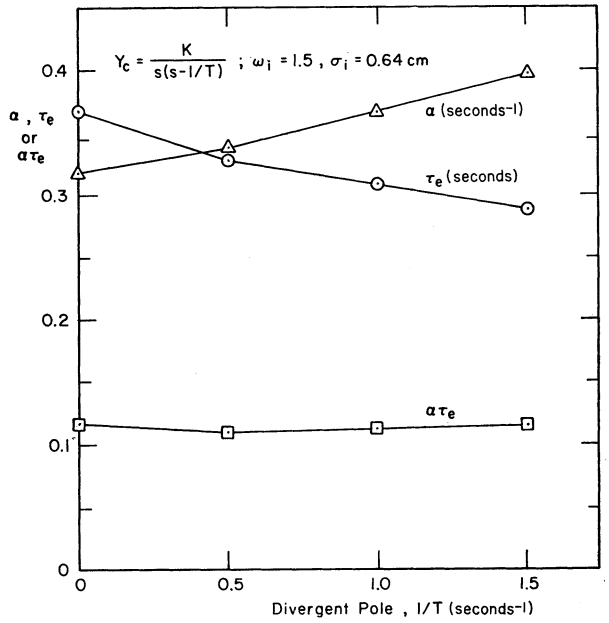

Fig. 7. Variation of α, τ_e, and $\alpha\tau_e$ with $1/T$.

The obvious improvement of the extended crossover model in fitting the previous data examples of Fig. 3 can be seen by comparing the dashed and solid lines therein. Its advantage in fitting marginally stable situations, for a second-order controlled element with one unstable root, $Y_c = K_c/s(s\text{-}1/T)$, is nicely illustrated in Fig. 6. Because the controlled element has a breakpoint in the crossover range $(1/T = 1.5)$ while the maximum lead equalization is required $(1/T_L \leq 0.2)$, it is not possible to achieve a —20 dB/decade amplitude slope near crossover, and the versatility of (9) is fully utilized.

The variation of α with task variables is not as well defined as ω_c and τ_e, chiefly because few valid data exist at low enough frequencies, and because the phase data at low frequencies have higher intrinsic variance. The best set of well-defined data for various degrees of instability of the above Y_c[19] results in the crossplot shown in Fig. 7. In this case, the product $\alpha\tau_e$ remained nearly constant at 0.11, but values from 0.04 to 0.20 have been observed.[30]

Constancy of $\alpha\tau_e$ implies that a favorable decrease in τ_e is accompanied by an adverse increase in α, such that the net phase curve due to α and τ_e has a constant concave-downward shape which merely shifts to a higher frequency on a Bode plot as τ_e decreases. The source of this close tie between α and τ_e involves details of the neuromuscular system which are discussed in references [31] and [32].

When the dynamics of the neuromuscular system lie in the crossover region, or when the manipulator feel characteristics are important, more elaborate models are required, e.g., the "precision model."[19] As the dynamics which contribute to the effective time delay of simpler models are separately accounted for in the more precise models, the minimum value of τ_e approaches the basic

system latencies and transport delays, and may be as low as 0.06 to 0.09 seconds.

With these simple models, the few rules, and the data of Figs. 3 and 4, remarkably good estimates can be made of the required pilot equalization, time delay, crossover frequency, stability margins, and tracking performance.

III. Remnant

A. Sources

Remnant is defined as the portion of the pilot's control output power which is not linearly correlated with the system input. Available measurements[19]–[21], [33] have shown that, for run lengths comparable to the time required to define the operator's describing function over a broad frequency band, the remnant signals have a continuous and smooth spectrum. The total output spectrum is thus the sum of two linearly uncorrelated spectra:

$$\Phi_{cc}(\omega) = |Y_p/(1 + Y_pY_c)|^2 \Phi_{ii}(\omega) + \Phi_{nn}(\omega) \qquad (10)$$

where

Φ_{cc} = total control output spectrum
Φ_{ii} = the input spectrum
Y_p, Y_c = pilot and controlled element describing functions
Φ_{nn} = "closed-loop" remnant spectrum.

In (10), Φ_{nn} represents signals which have been passed around the loop, i.e., it is the closed-loop remnant. To ascribe this closed-loop spectrum to processes internal to the pilot requires opening the loop and computing the signal properties which would have to be present at the specified places to yield the total closed-loop spectrum. In general, the sources of remnant are impossible to describe uniquely using only two-terminal measurements. As matters stand at present, one can only attempt to list and, by indirect measurement, to infer the dominant sources and most usable remnant models for a particular set of task variables. In ascending order of importance, the sources of remnant are considered to be due to the following.

1) *Pure Noise Injection:* There are numerous potential sources of legitimate "noise" along the sensing, equalizing, and actuating paths of the human pilot; for example, errors in the output position similar to the "range effect"[34] but on a continuous basis.[20], [21]

2) *Nonlinear Operations:* Nonlinearities such as indifference thresholds, control output and rate saturation, or relay-like "sgn" functions produce harmonics of frequencies other than input frequencies, although their dominant (fundamental) effect is taken into account by the describing function. If the nonlinearities are large compared with the signal levels involved, then appreciable remnant can result from this source.[21], [35], [36]

3) *Nonsteady Pilot Behavior:* The parameters of the quasi-linear pilot model can be defined meaningfully only as averages over certain lengths of time.[37] However, there is increasing evidence that significant time variations in the pilot's parameters occur during tracking, with variations in pilot gain and time delay as the prime offenders.[19], [38]–[40]

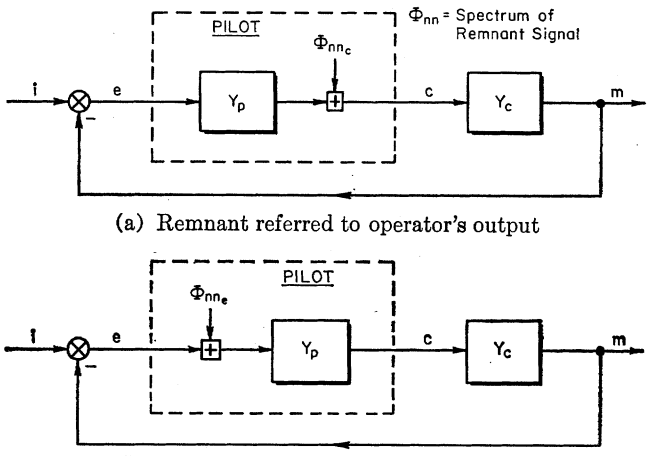

(a) Remnant referred to operator's output

(b) Remnant referred to operator's input

Fig. 8. Block diagrams for remnant model.

B. Model

Clearly, the most appropriate way to treat remnant effects depends on the actual component sources present. When, however, mean-squared values of signals within the control loop are of central interest, the remnant can be satisfactorily represented by a signal having a specified power spectral density injected into the closed-loop system (see Fig. 8).

Considered as an injected signal, the point of application of the remnant can be removed from the pilot's output to other locations in the loop as long as no nonlinear elements are passed in the process. In other words, the remnant may be considered to be injected at the pilot's output, input, or somewhere in between (if such pilot nonlinearities as the indifference threshold are negligible). Referring to Fig. 8 and denoting the injected remnant at e and c in the loop as Φ_{nn_e} and Φ_{nn_c}, respectively, the various remnant forms are related by

$$\Phi_{nn} = \frac{\Phi_{nn_c}}{|1 + Y_pY_c|^2} = \frac{\Phi_{nn_e}|Y_p|^2}{|1 + Y_pY_c|^2}. \qquad (11)$$

C. Data

Remnant data are far more sparse than describing function information, and the data available are not especially reliable. McRuer *et al.*[19] have supplied new data on the remnant which are not definitive but have resulted in considerable refinement to the above ideas. These new findings show the following results.

1) Careful examination of the output power spectral density indicated no evidence for periodic sampling[41], [42] or strongly nonlinear behavior. Many of the long runs (4 minutes) of McRuer *et al.*[19]

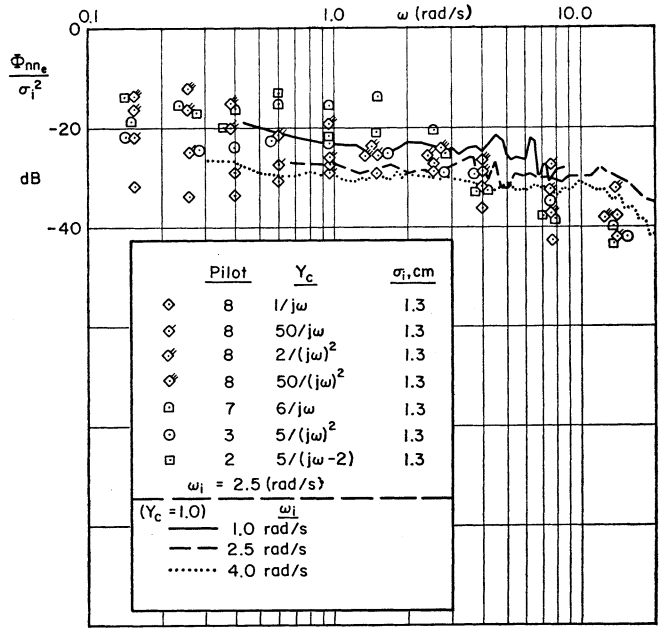

Fig. 9. Typical remnant power spectra for various controlled elements.[19], [20]

from which this statement derives have recently been re-examined for intervals as short as 20 seconds with the same conclusion. It is important to note, however, that random or other nonperiodic sampling behavior[43], [44] is not ruled out as a possibility.

2) At low frequencies, the remnant data for a wide variety of controlled elements coalesce best when all the remnant is injected at the pilot's input.
3) Remnant increases with controlled element gain, with forcing function bandwidth, and with control order.
4) Some evidence for pulsing behavior in control of second-order controlled elements is indicated by output amplitude distributions. These indicate a tendency for the pilot's output to be pulse areas roughly proportional to the stimulus amplitude, when maximum lead equalization is used.

Some typical remnant spectra from McRuer *et al.*[19] are given in Fig. 9 for a variety of controlled elements. Also shown are curves adapted from Elkind[20] for $Y_c = 1$.

The measurement and modeling of remnant is an area requiring sophisticated equipment and techniques, and much work remains to be done.

IV. Single-Axis Pursuit Model

Often the pilot has some knowledge of the forcing function, either directly (as on a separate display) or by implication (due to perceived patterns in the error displays or in his control action). The vehicle output is also frequently available to the pilot (e.g., as motion relative to the horizon). The error is still available as the perceived difference between input and output. This is a "pursuit" tracking situation, which is formally distinguished from the compensatory case by the addition

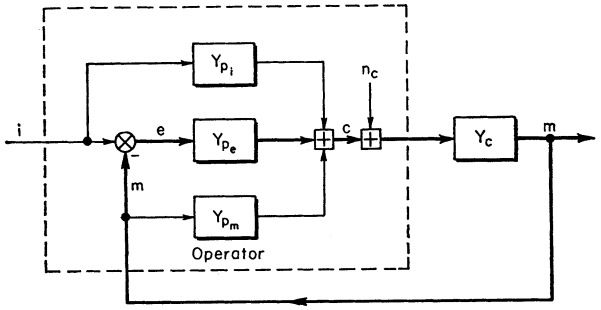

Fig. 10. Block diagram for the pursuit model.

of the feedforward loop containing the block Y_{p_i} and the direct feedback of output via the block Y_{p_m} to describe the pilot's actions. These are shown in Fig. 10.

The Y_{p_i} operation represents an essentially open-loop feedforward response to the input, Y_{p_m} represents a closed-loop operation on the output, and Y_{p_e} represents the closed-loop operation on the error, as before. Those functions, which are typically internal to the operator, are enclosed by a dashed line in Fig. 10, including the differential which produces the error e. In the alternative case where e and m are available, i may be inferred by the the operator.

Recent experimental activities[45] have resulted in a better understanding of pursuit behavior. One explanation of these results is that the operation on the error Y_{p_e} is much the same as the quasi-linear describing function for compensatory tracking, and that the operator does use his additional knowledge of the forcing function to improve performance via Y_{p_i}. Operations in which Y_{p_m} is likely to be important are thought to be those involving motion cues, but this has not yet been clearly demonstrated.

The best strategy in pursuit tracking may be assessed by considering the closed-loop errors (and assuming Y_{p_i} to be a quasi-linear operation). Straightforward block diagram algebra, based on Fig. 10, gives the system error spectrum (with $Y_{p_m} = 0$),

$$\Phi_{ee}(\omega) = \frac{(1 - Y_{p_i}Y_c)\Phi_{ii} - \Phi_{nn_c}Y_c}{1 + Y_{p_e}Y_c}. \tag{12}$$

It can be seen that in the absence of remnant Φ_{nn_c}, the input tracking errors theoretically can be made to vanish by making $Y_{p_i} = 1/Y_c$. There is always some disturbance or remnant internal to the loop, however, and the errors due to this source are minimized by the same strategy as for conventional compensatory tracking described in Section II. Furthermore, it is the Y_{p_e} loop which determines the closed-loop stability of the system, so this loop *must* be closed if the vehicle is unstable.

It is difficult to experimentally determine Y_{p_i} and Y_{p_e} (or Y_{p_m}) because the responses from these "boxes" are not separately available outside the operator. Consequently, only a few describing function measurements of this type exist, and these are not comprehensive enough to assess the laws of adaptation as was done in Section II. However, some of the data of Wasicko *et al.*[45] do indicate

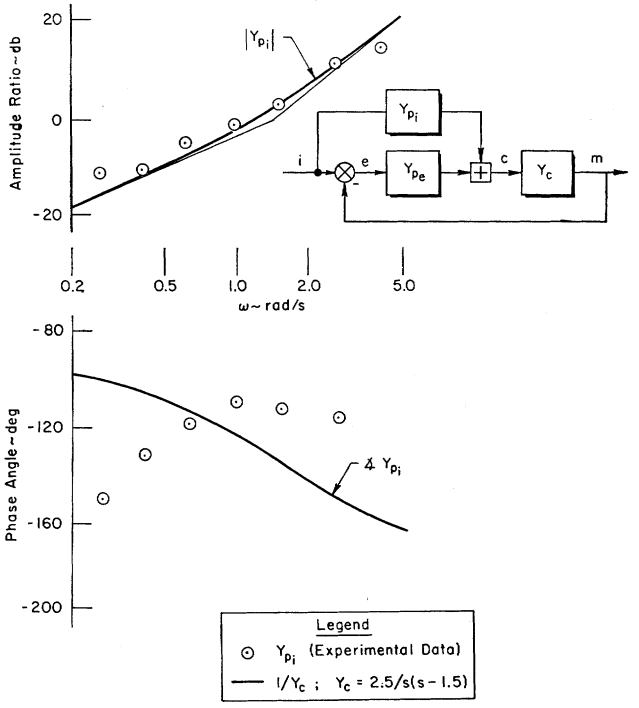

Fig. 11. Indirectly measured pilot feedforward describing function.[45]

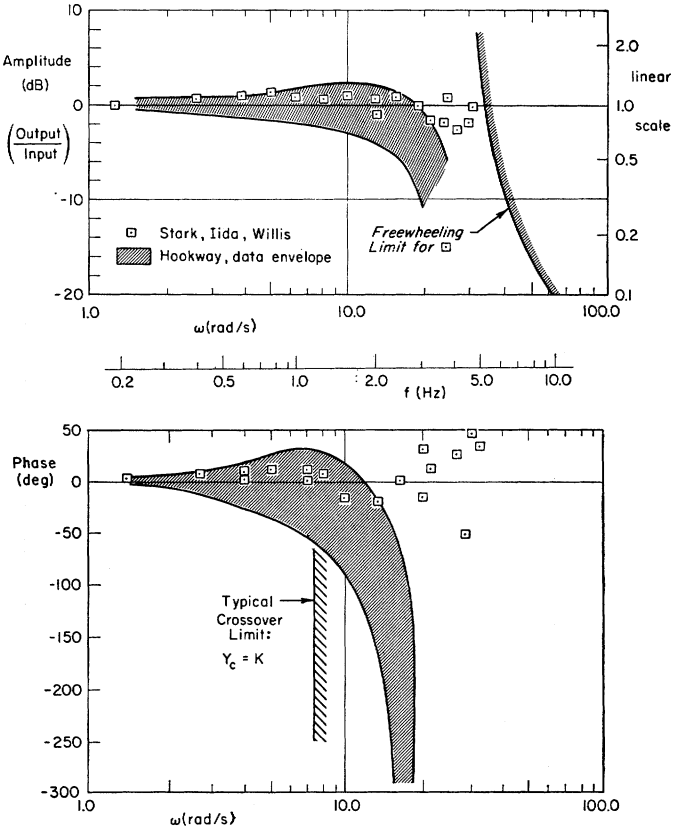

Fig. 12. Frequency response data for a single sinewave input at various frequencies.[51] [53]

that the adjustment of Y_{p_i} is nearly $|Y_{p_i}Y_c| \doteq 1$ over a fairly broad frequency range. In other words, the system becomes nearly open-loop through the feedforward, with the feedback acting as a vernier control and as a means of stabilizing the controlled element when needed.

An excellent example of pursuit activity is given in Fig. 11, which shows the implied Y_{p_i} generated in control of a second-order system with an unstable divergence, under the assumption that Y_{p_e} is the same as it was for an error-only display. The degree to which the ideal $Y_{p_i}Y_c = 1$ seems to be approached is remarkable for the amplitude ratio, although nowhere near as close in phase. Further measurements of pursuit behavior are given in Elkind[20] and Wasicko *et al.*[45]

V. Model for Periodic Forcing Function

A. Background

A model for the pilot's response to a periodic forcing function is of considerable interest for the analysis of pilot-induced oscillations (PIO), during which large and distinct sinusoidal motions dominate the pilot's input.[46], [47] Periodic stimuli also exist while attempting to follow the optical landing beam of an aircraft carrier being subjected to heavy swell[48] or in following some types of rolling terrain. Certain types of clear-air turbulence give rise to strongly periodic disturbances.

Periodic inputs to the pilot will yield different forms of pilot response than unpredictable inputs. Under favorable conditions, the skilled operator is able to detect such periodicities within one or two cycles and to take advantage of this knowledge in an attempt to achieve better performance. The operator's response to a particular set of sinusoidal inputs can be presented on a frequency response plot, but it must be recognized as an ensemble of responses to single frequencies, and that different psychomotor mechanisms may be involved in the low, medium, and high-frequency ranges.

B. Data Base

A large number[49]-[54] of periodic-wave tracking studies exist, almost all for $Y_c = K_c$. Fig. 12 shows two sets of these data[51], [53] plotted versus frequency. It is apparent that up to about 8 rad/s, the output/input is nearly unity with very small phase errors. Beyond this frequency, the phase data are erratic and the amplitude shows increasing attenuation up to the "freewheeling" limit of about 30 rad/s, as shown by the shaded boundary in Fig. 12. Early experiments by Ellson and Gray[49] and recent, very complete studies by Vossius[52] shed further light on the scattered phase data. Their data show that up to about 20 rad/s the output *frequency* follows the input frequency, but beyond this, the output *frequency* actually exceeds that of the input up to the frequency of neuromuscular limiting. Thus the region of erratic phase data of Stark *et. al.*[51] and Muckler *et al.*[53] and of nonidentical frequency data of Ellson and Gray[49] and Vossius[52] coincide. The interpretation is that large

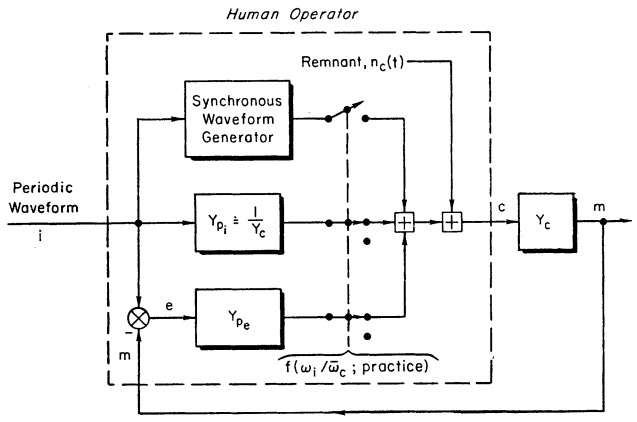

Fig. 13. Block diagram for periodic waveform model.

randomly varying phase angles can be interpreted as frequency changes, and *vice versa.*

C. Model

The model derived from these data, as well as the observations of other experimenters, e.g., Pew *et al.*,[54] is shown in Fig. 13 and is described as follows.

1) For periodic inputs up to about 10 rad/s (2 Hz), the operator creates a pursuit feedforward loop in which $Y_{p_i}Y_c \doteq 1.0$, which serves to eliminate all of the time-averaged lags from his tracking. However, remnant will still excite residual errors, so a compensatory loop is also maintained, subject to similar laws of adaptation as in the random input case for very low frequency inputs. The result will be one peak in the perceived error spectrum near the input frequency and, possibly, a secondary peak near the crossover frequency.

2) As familiarity with a particular waveform increases, Y_{p_i} takes on the form of a synchronous waveform generator which is phase locked to the zero crossings of the input or error. Thus, the operator's behavior becomes more and more open loop, or preprogrammed, and the errors at the input frequency will decrease.

3) For inputs between about 10 and 30 rad/s (2 to 5 Hz), the operator can no longer close the compensatory loop effectively, so crossover regression (or even complete opening of the compensatory loop) occurs. Even though the synchronous generator produces a reasonable waveform, it is no longer phase locked to the input frequency, so continuous phase shifting or frequency drifting can occur.

4) The maximum periodic frequency is limited by the basic neuromuscular dynamics of the limb plus control stick, which also limits the sharpness in reproducing periodic square or triangular waveforms.

In short, the periodic waveform tracking model is a near-perfect pursuit model, in which $Y_{p_i}Y_c \doteq 1.0$ *up to* $\omega_{c_{max}}$; *and an open-loop model from* $\omega_{c_{max}}$ *to the neuromuscular cutoff frequency.*

The achievement of synchronous waveform generation can be tested by having the operator close his eyes while

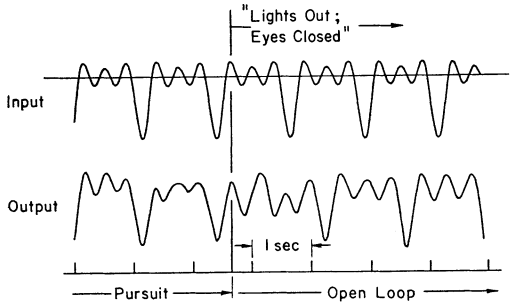

Fig. 14. Demonstration of synchronous pattern generation.[52]

continuing to operate his control stick as before. The visual loop is thereby opened and the control action results solely from continuation of the internally generated pattern. Fig. 14, taken from Vossius,[52] illustrates this precognitive level of control very nicely. Notice that prior to "lights out, eyes closed," the three-wave output is exactly in phase but distorted by the residual tracking errors. After "eyes closed" the waveform is nearly perfect (after an initial transient) but considerably out of phase with the input. Further illustrations of synchronous tracking of complex periodic outputs are given in McRuer and Krendel[21] and Hess.[55], [56]

This model is consistent with the previous compensatory and pursuit models, and with the Successive Organization of Perception concept in Krendel and McRuer.[57] Although direct validation of this model has not yet been obtained, it does explain most of the extant data and several of the qualitative features and anomalies observed during periodic waveform tracking (e.g., Pew *et al.*[54]).

VI. Multiloop Compensatory Model

A. Types of Multiple-Loop Tasks

As used here, the term "multiloop" refers to two or more *interacting* loops, while control tasks involving noninteracting loops are referred to as "multiple loop." For example, pitch angle and height control is a multiloop task, while pitch and bank angle stabilization in straight and level flight is a multiple-loop task. Multiloop tasks involve, in general, more than one feedback quantity (e.g., pitch angle and height) as well as one or more different pilot controls (e.g., elevator and throttle).

The inputs to the pilot may be perceived by only one of the senses (single modality) or by several senses (multimodality). Fixed-base simulation nearly always is limited to the single-modality case, e.g., visual cues only; motion simulators and actual flight involve the multimodality situation, e.g., visual and motion cues. The main justification for ignoring the nonvisual aspects in many pilot-vehicle analyses is that the visual cues have been found, empirically, to dominate the pilot's response, and they yield results which seem to be valid. However, there are several important exceptions, among which are:

pilot-induced oscillations, gust suppression, elastic mode vibrations, mass-overbalanced controls, bobweight effects, and spurious motion simulation effects. However, multimodality pilot models are in a primitive state of development, and few definitive experiments have been performed to isolate the cues and criteria for such models.

Practical control engineering techniques for analyzing pilot-vehicle multiloop problems for systems of moderate complexity have recently been developed[58], [59] and applied to aircraft manual control and handling qualities.[60]–[62] The pilot model to be described next applies to either multiloop or multiple-loop tasks, as long as essentially continuous control is being exerted in each loop.

B. The Adaptive Feedback Selection Hypothesis

The pilot model for multiloop tasks is an extension of the quasi-linear describing function model for single-loop tasks, but with different parameters operating in each loop. Whereas the tradeoffs between performance, stability, and pilot equalization effort are relatively clear-cut in single-loop situations, the number of alternatives becomes much greater in multiloop systems. To converge on the probable feedbacks and equalization selected by the pilot, the Adaptive Feedback Selection Hypothesis has been formed, which is based on considerable indirect evidence, but has yet to be completely validated.

Adapative Feedback Selection Hypothesis

Given: A controlled element having several degrees of freedom, some directly sensed within the general visual field, some observable via visual displays, and (perhaps) some directly sensed using modalities other than vision.

Then: The human pilot evolves, during a learning and skill development phase, a particular multiloop system structure. The active feedback connections in this system will be similar to those which would be selected by a skilled controls designer who has available certain variable system characteristics to use for control of given fixed system characteristics; and who also has available a relative preference guide for the variables. System variables comprise sensing channels for each of the feedback possibilities available to the pilot, and possible equalization in each loop which is tailored from an adaptive, but limited, set of equalization forms.

The loops ultimately selected will have the following properties.

1) To the extent possible, the feedback loops selected and equalizer adjustments made will be such as to allow wide latitude and variation in pilot characteristics.

2) The loop and equalization structure selected will exhibit the highest pilot rating of all practical loop closure possibilities. Preferably, the loops selected can be closed with a pure gain plus large time delay.

3) Delays due to scanning and sampling are minimized.

C. Adjustment Rules

1) *Outer Loops:* The outer loop is equalized in accordance with the single-loop rules given in Section II with some additions to account for the closure of other (inner or parallel) loops.

a) *Equalization:* The equalization form and parameters are based on the "effective controlled element" with the inner loops closed, i.e., the outer-loop Y_c includes the augmenter-like action of the pilot in the inner loop. In general, feedback selections which involve much equalization, or different equalization in each loop, seem to be avoided by the pilot. A wide range of acceptable outer loop gains is desirable.

b) *Effective Time Delay:* When several displays must be sampled, an additional increment, T_s equal to the effective time delay due to sampling behavior, is added to τ_0.

c) *Crossover Frequency:* The same crossover frequency considerations apply as for the single-loop case. Often the outer loop has a lower crossover frequency than the inner-loop or single-loop cases because of a larger accumulation of effective time delays.

2) *Inner Loops:* Ordinarily the inner loops act as equalization for subsequent loops, or provide feedbacks or crossfeeds which suppress subsidiary degrees of freedom which have undesirable effects on subsequent loops. Because the role of the inner loops is so dependent on outer loop requirements, the rigid rules given above for the outer loop are not generally applicable, e.g., even stability may not be required. The types of inner loops closed and the equalization selected will generally be compatible with one or all of the following considerations.

a) Outer loop adjustments per the single-loop adjustment rules become more feasible, e.g., $|Y_pY_c|$ can be made approximately —20 dB/decade with less outer-loop equalization.

b) The sensitivity of the closed-loop characteristics to changes in either inner or outer-loop pilot characteristics is reduced from that in an outer-loop-only situation. This includes the improvement of gain and phase margins.

c) The loop structure and equalization selected are those for which total pilot rating is the best obtainable.

d) Sampling penalties are minimized.

D. Example

Insufficient data have been obtained to validate these selection and adjustment rules completely, but an example will be given of the pilot's describing function in a simulated multiloop task involving manual control of roll and yaw with ailerons and rudder.[59] By being given an aircraft with a dynamically unstable Dutch roll

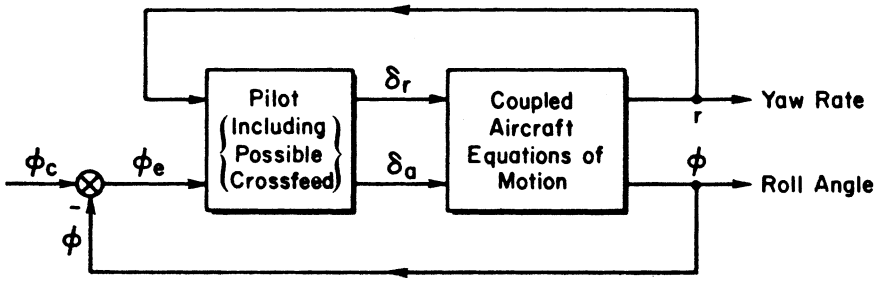

(a) Block diagram

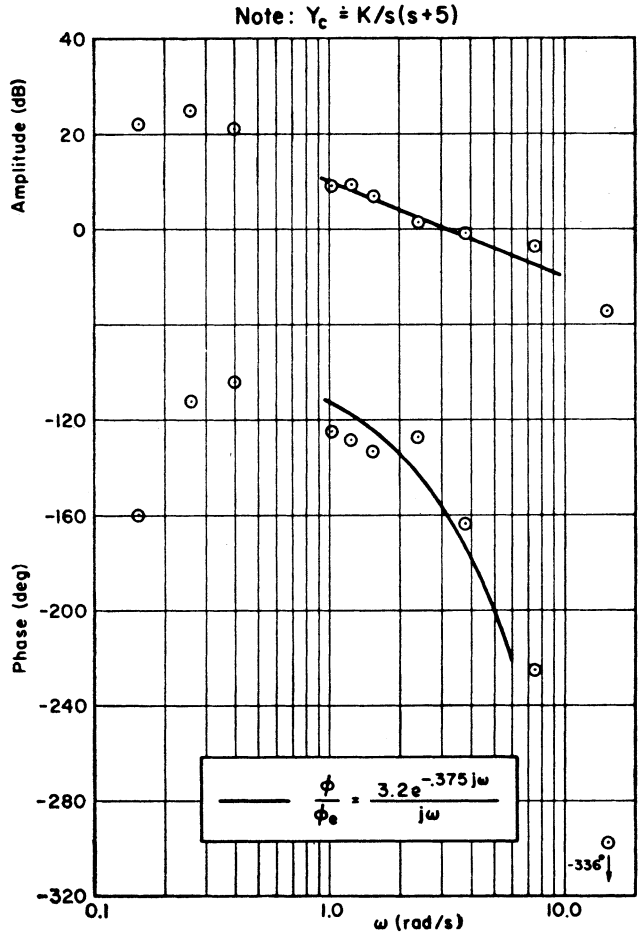

(b) Aileron control only (stable yaw axis)

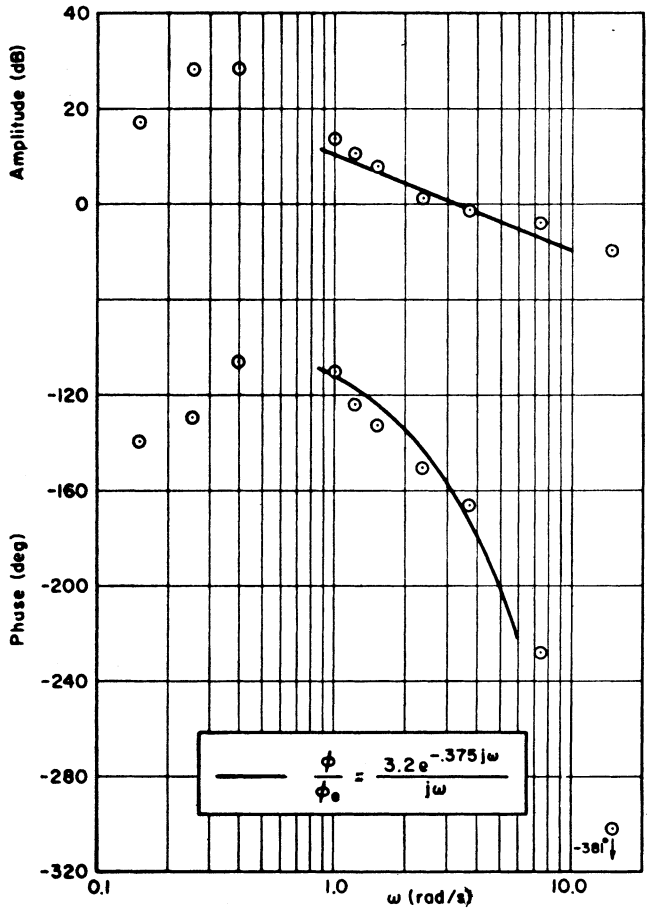

(c) Aileron-plus-rudder control (unstable yaw axis)

Fig. 15. Comparison of single-loop and multiloop describing functions for a roll tracking task.[59]

mode, the pilot was forced to use rudder to control yaw rate, and by being given a large random roll command he was forced to control roll by ailerons (compensatory displays were used). The block diagram for this situation is depicted in Fig. 15(a). One question was whether much crossfeed existed between roll or yaw errors and the rudder or aileron control actions, and another was the extent of change in the pilot's roll-to-aileron describing function from its single-loop equivalent.

It was found that there was some roll-to-rudder crossfeed which prevented direct measurement of the yaw-to-rudder describing function. However, the roll-to-aileron describing function was measured. The inner-loop closure and crossfeed for the unstable case were such that the pilot's roll-to-aileron describing function in the multiloop task [Fig. 15(c)] was the same as it was for a stable Dutch roll mode, in which case he had to close only the single loop, roll-to-aileron [Fig. 15(b)].

Summarizing, then, it appears that numerous multiloop piloting tasks can be modeled with simple extensions of the well-established single-loop model. The potential applications of pilot models are thereby vastly expanded and the need for sophisticated multiloop experiments and data interpretation is, indeed, acute.

VII. Pilot Rating Considerations

A. Single-Axis

1) *General Factors:* In the iterative process of determining the likely loop structure and loop equalizations, the key adaptation criteria are not always confined to the objective measures of stability margins and error performance; they also include consideration of subjective pilot ratings.[63] Although the connections between pilot ratings and pilot-vehicle dynamics and performance are not yet firmly established, enough are available to provide a relative preference guide (e.g., see reference [64]. This brief discussion summarizes only those pilot rating considerations which affect the pilot's adaptation and is not intended to be definitive in any sense.

The whole pilot adaptation problem is complicated by the fact that the adopted parameters and performance affect his ratings, and vice versa. Consequently, most of the trends to be shown in the following figures were measured under conditions where all but one of the variables affecting rating were constant or negligible.

2) *Pilot Gains:* The subjective rating trends associated with the controlled element gain are the best known, for numerous experiments have shown that an "optimum" gain exists at some level of K_c. The importance of the optimum gain is illustrated in Fig. 16, which shows results from a single-axis compensatory tracking study which used "good" airplane dynamics.[65] Over a wide range of control gains, the average absolute error is nearly constant, while the pilot's average force output (proportional to pilot gain) varies inversely with the control gain. The subjective handling quality rating shows a distinct optimum, which is not revealed by either the error or force criteria. All of these trends are consistent with the pilot's gain adaptation to keep ω_c invariant.

Fig. 17(a) presents pilot rating versus controlled element gain curves obtained from several sources.[65]–[67] Of interest are the rather broad gain optimums (1.0-point decrement over a 300 to 400 percent range of K_c) and the severe degradation of rating for higher and lower gains. To the extent that the crossover model applies to the case at hand and ω_c is constant, Fig. 17(b) can be used to roughly estimate the penalties for off-optimum pilot gain once ω_c is known via the relation

$$K_p \doteq \frac{\omega_c}{K_c} \tag{13}$$

where K_c includes the vehicle and display gains.

The absolute level of the optimum control gain will depend on manipulator characteristics and other mission and control sensitivity considerations (e.g., see A'Harrah and Siewert[46]). At the present state of the art, the "best" control gains must still be empirically determined.

3) *Pilot Lead and Lag:* Ashkenas[68] contains an extensive study, based on ground and flight tests from a number of sources, of pilot ratings for a general class of

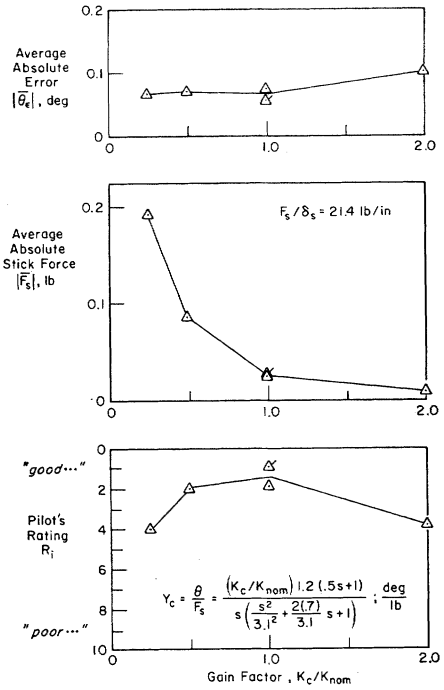

Fig. 16. Typical performance measures and ratings versus gain for a "good" controlled element.[65]

vehicles wherein $Y_c \doteq K_c/s(Ts + 1)$. The control gain was generally optimum and errors were small, so both were eliminated as factors in pilot rating. This left T_L as the primary factor influencing rating. As shown in Table II, for this type of controlled element the pilot adopts a lead which nearly cancels the lag; i.e., $T_L \doteq T$. Fig. 18 is the resulting plot of the effects of T_L on pilot rating; the vertical spread in the points is due to uncertainties in the exact value of T_L. Similar variations may be inferred from the results given in Ashkenas and McRuer.[22] Nevertheless, great caution should be used in attributing the rating decrements of Fig. 18 entirely to pilot lead, because so many factors were not in control.

The effect of pilot-adopted *lag* on his ratings has not been found as yet. Indirect evidence (e.g., the static-to-short-period-gain experiment in Jex and Cromwell[65]) indicates that the use of very-low-frequency lag—in effect, the trimming out of drift errors—does not result in significant rating penalties. However, there is a growing suspicion that vehicles which *require* mid- to high-frequency pilot lags, in order to attenuate or phase-stabilize a weakly damped short-period or bending mode, may be downrated on this basis.

4) *Effective Time Delay:* It has been suggested in previous sections that the pilot can reduce his effective time delay τ_e by reducing the neuromuscular lags. As an unpublished facet of the experiments in McRuer *et al.*,[19] pilot ratings were recorded for the unstable element, $Y_c = K_c/s(s - 1/T$. As $1/T$ was increased, the effective time delay was reduced. Since ω_c and the errors were observed to remain constant, and the lead was constant at very low frequencies, the observed rating decrement can be attributed to $\Delta\tau_e$. Specifically, as the unstable root

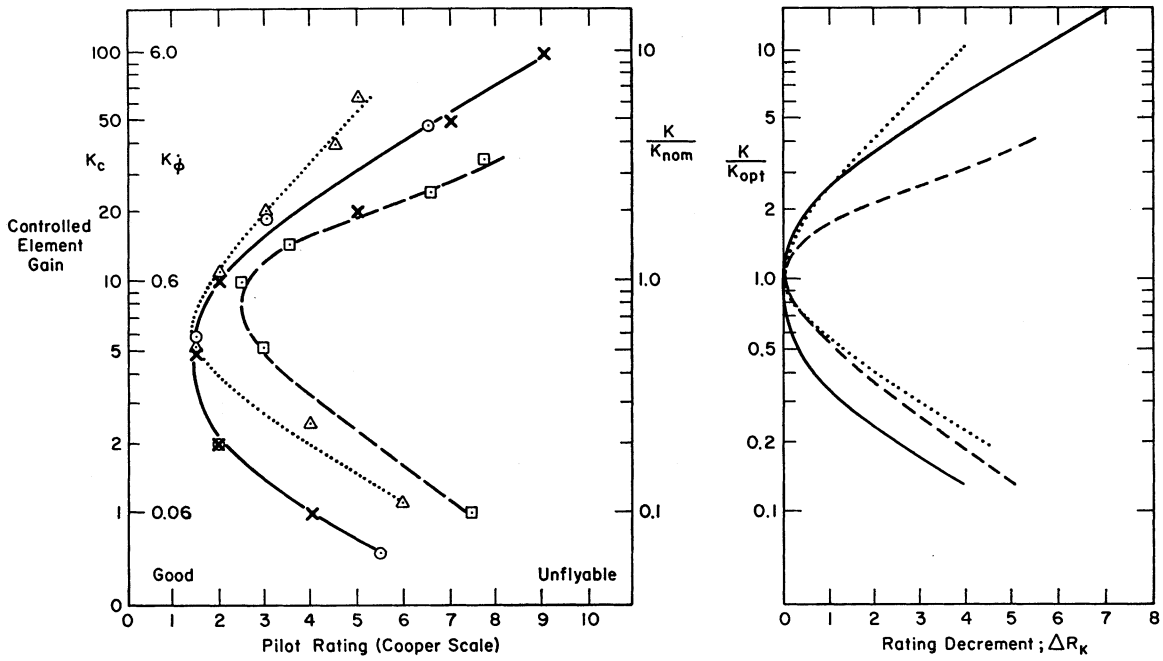

(a) Basic data (b) Normalized decrement

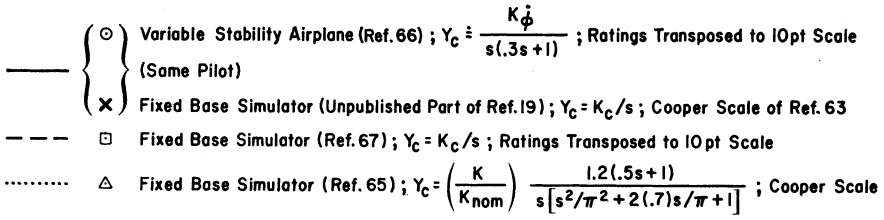

Fig. 17. Pilot ratings versus controlled element gain.

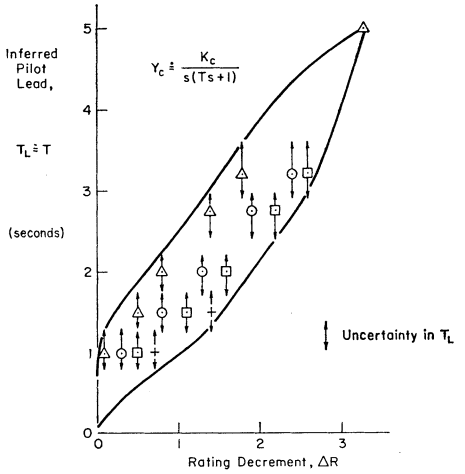

Fig. 18. Rating decrement due to pilot lead as inferred from handling qualities tests[68] (symbols refer to various cases within the reference).

went from 0 to 1.5 rad/s, τ_e underwent a reduction of 0.08 seconds and the pilot rating dropped by 2.5 to 3 points. This rating decrement is probably associated with the increasing neuromuscular tension underlying the reduced τ_e.

5) *Other Factors:* Other things being constant, pilot ratings may also depend on the system closed-loop performance and the sensitivity of the performance to variations in elements of the pilot's describing function. For good ratings, the pilot should be able to obtain satisfactory performance with a relatively broad set of describing function characteristics.

The influence of remnant on pilot rating is not understood at all, although it has been observed[19] that the proportion of remnant in the control output does increase in the high control gain region of Fig. 17 (i.e., for $K_c > 10$).

B. Multiaxis Ratings

The above rating penalties are based on single-axis data. A simple approximation to the total system rating can be made using a "basic" experimentally determined multiaxis rating and adding single-axis rating decrements:[69]

$$R = R_{m_{best}} + \sum_{i=1}^{N} \Delta R_i \qquad (14)$$

where

$R_{m_{best}}$ = actual pilot rating for the multiaxis situation when each single axis is set to its best-rated configuration (experimentally determined)

ΔR_i = rating decrement (relative to the optimum) for each of the axes involved, based on single-axis rating data.

Other multiloop rating considerations are also discussed in Dander.[69]

In summary, it can be seen that subjective pilot ratings may have a strong influence on his finally adopted parameters, and vice versa.

VIII. Conclusions

This paper has attempted to summarize some of the more important recent developments in analytical pilot models for manually controlled vehicles, with emphasis on the effects of task variables on the types of models required and on the model parameters. Some of the main conclusions which emerge from this review are as follows.

1) Validated analytical pilot models are available for a wide range of task variables.

2) To handle the wide range of problems, different *forms* of pilot models are required (e.g., compensatory, pursuit, periodic, etc.). The extra blocks in these models must not be overlooked, as they sometimes are, in interpreting simulator and flight test data.

3) Great simplifications in the modeling of compensatory tasks result from using the Crossover Model or its refinements described in Section II. These permit prediction of pilot equalization, gain, delay time, performance, and rating decrements.

4) Multiloop tasks lead to models similar to those for single-loop tasks, and most of the adaptation rules seem to be equally valid. The Adaptive Feedback Selection Hypothesis of Section VI appears to be a powerful rule for selecting the most useful display quantities from an array of possibilities.

5) Much more work needs to be done in the understanding and modeling of pilot remnant.

6) A pilot's rating decrements can be related to his adopted model parameters, thereby permitting better optimization of the pilot-vehicle system than can be obtained solely on the basis of stability or performance criteria.

Acknowledgment

Numerous colleagues, at Systems Technology, Inc., and elsewhere, have played a major role in developing the pilot models reported herein. The authors would like to especially acknowledge the contributions of I. L. Ashkenas, F. D. Graham, E. S. Krendel, R. E. Magdaleno, W. Reisener, Jr., R. L. Stapleford, and R. J. Wasicko.

References

[1] D. T. McRuer and E. S. Krendel, "The human operator as a servo system element," *J. Franklin Inst.*, vol. 267, pp. 381–403, May 1959; pp. 511–536, June 1959.

[2] J. C. R. Licklider, "Quasi-linear operator models in the study of manual tracking," in *Developments in Mathematical Psychology*, R. D. Luce, Ed. Glencoe, Ill.: Free Press, 1960, pp. 169–279.

[3] T. B. Sheridan, "The human operator in control instrumentation," in *Progress in Control Engineering*, vol. 1, R. H. Macmillan *et al.*, Eds. New York: Academic Press, 1962, pp. 141–187.

[4] J. I. Elkind, "A survey of the development of models for the human controller," in *Guidance and Control*, vol. 2, R. C. Langford and C. J. Mundo, Eds. (*Progress in Astronautics and Aeronautics*, vol. 13.) New York: Academic Press, June 1964, pp. 623–643.

[5] L. G. Summers and K. Ziedman, "A study of manual control methodology with annotated bibliography," NASA CR-125, November 1964.

[6] L. R. Young and L. Stark, "Biological control systems—A critical review and evaluation," NASA CR-190, March 1965.

[7] D. T. McRuer and I. L. Ashkenas, "Applied pilot-aircraft control theory," presented to AGARD Ad Hoc Panel on Guidance and Control, Symp. on the Human Operator and Aircraft and Missile Control, Paris, September 1966.

[8] R. G. Costello and T. J. Higgins, "An inclusive classified bibliography pertaining to modeling the human operator as an element in an automatic control system," *IEEE Trans. Human Factors in Electronics*, vol. HFE-7, pp. 174–181, December 1966.

[9] A. Tustin, "The effects of backlash and of speed dependent friction on the stability of closed-cycle control systems," *J. IEE (London)*, pt. 2a, vol. 94, pp. 143–151, 1947.

[10] R. J. Kochenburger, "A frequency response method for analyzing and synthesizing contactor servomechanisms," *Trans. AIEE*, vol. 69, pp. 270–283, 1950.

[11] D. Graham and D. McRuer, *Analysis of Nonlinear Control Systems*. New York: Wiley, 1961.

[12] K. Chen, "Quasi-linearization techniques for transient study of nonlinear feedback control systems," *Trans. AIEE*, pt. 2, vol. 75, pp. 354–363, 1956.

[13] R. C. Booton, Jr., "The analysis of nonlinear control systems with random inputs," *Proc. Symp. on Nonlinear Circuit Analysis*, vol. 2, Polytechnic Institute of Brooklyn, 1953, pp. 369–391.

[14] ——, "Nonlinear control systems with random inputs," *IRE Trans. Circuit Theory*, vol. CT-1, pp. 9–18, 1954.

[15] M. Sadoff, "Effects of high sustained acceleration on pilots'

performance and dynamic response," NASA TN D-2067, July 1964.

[16] M. Sadoff and C. B. Dolkas, "Acceleration stress effects on pilot performance and dynamic response," *2nd Ann. NASA-University Conf. on Manual Control,* NASA SP-128, pp. 241–258, 1966.

[17] A. Z. Weisz, R. W. Allen, and C. J. Goddard, "An evaluation of three types of hand controllers under random vertical vibration," *2nd Ann. NASA-University Conf. on Manual Control,* NASA SP-128, pp. 269–278, 1966.

[18] D. McRuer and D. Graham, "Pilot-vehicle control systems analysis," in *Guidance and Control,* vol. 2, R. C. Langford and C. J. Mundo, Eds. New York: Academic Press, June 1964.

[19] D. McRuer, D. Graham, E. Krendel, and W. Reisener, Jr., "Human pilot dynamics in compensatory systems—theory, models, and experiments with controlled element and forcing function variations," AFFDL-TR-65-15, January 1965. (Condensed version in *J. Franklin Inst.,* vol. 238, January-February, 1967.)

[20] J. I. Elkind, "Characteristics of simple manual control," M.I.T. Lincoln Lab., TR111, April 1956.

[21] D. T. McRuer and E. S. Krendel, "Dynamic response of human operators," WADC-TR-56-524, October 1957.

[22] I. L. Ashkenas and D. T. McRuer, "The determination of lateral handling quality requirements from airframe/human-pilot system studies," WADC-TR-59-135, June 1959.

[23] H. R. Jex, J. D. McDonnell, and A. V. Phatak, "A 'critical' tracking task for man-machine research related to the operator's effective delay time—I: Theory and experiments with a first-order divergent controlled element," NASA CR-616, October 1966.

[24] T. E. Leonard, "Optimizing linear dynamics for human-operated systems by minimizing the mean square tracking error," *IRE WESCON Rec.,* vol. 4, pt. 4, pp. 57–62, 1960.

[25] J. I. Elkind and D. C. Miller, "On the process of adaptation by the human controller," presented at the IFAC Meeting, London, 1966.

[26] R. W. Obermayer, R. B. Webster, and F. A. Muckler, "Studies in optimal behavior in manual control systems: The effect of four performance criteria in compensatory rate-control tracking," *2nd Ann. NASA-University Conf. on Manual Control,* NASA SP-128, pp. 311–324, 1966.

[27] J. Wolkovitch and R. Magdaleno, "Performance criteria for linear constant-coefficient systems with random inputs," ASD-TDR-62-470, January 1963.

[28] R. W. Obermayer, R. B. Webster, and F. A. Muckler, "Research study on optimal manual control systems," Bunker-Ramo Corp., Final Rept., June 15, 1966.

[29] D. T. McRuer and E. S. Krendel, "The man-machine system concept," *Proc. IRE,* vol. 50, pp. 1117–1123, May 1962.

[30] J. D. McDonnell and H. R. Jex, "A 'critical' tracking task for man-machine research related to the operator's effective delay time—II: Experimental effects of system input spectra, control stick stiffness, and controlled element order," NASA CR-674, January 1967.

[31] D. McRuer, "Remarks on some neuromuscular subsystem dynamics," *IEEE Trans. Human Factors in Electronics,* vol. HFE-7, pp. 129–130, September 1966.

[32] D. T. McRuer, R. E. Magdaleno, and G. P. Moore, "A neuromuscular actuation system model," presented at the 3rd Ann. NASA-University Conf. on Manual Control, March 1967; to be published as a NASA Special Publication.

[33] A. Tustin, "The nature of the operator's response in manual control and its implications for controller design," *J. IEE (London),* pt. 2a, vol. 94, 190–202, 1947.

[34] C. W. Slack, "Some characteristics of the 'range effect'," *J. Exp. Psychol.,* vol. 46, 1953.

[35] Goodyear Aircraft Corp., "Investigation of control "feel" effects on the dynamics of a piloted aircraft system," Rept. GER-6726, April 25, 1955.

[36] N. D. Diamentides, "A pilot analog for airplane pitch control," *J. Aeronaut. Sci.,* vol. 25, pp. 361–370, June 1958.

[37] W. W. Wierwille, "A theory for optimal deterministic characterization of time-varying human operator dynamics," *IEEE Trans. Human Factors in Electronics,* vol. HFE-6, pp. 53–61, September 1965.

[38] J. D. McDonnell, "A preliminary study of human operator behavior following a step change in the controlled element," *IEEE Trans. Human Factors in Electronics (Communication),* vol. HFE-7, pp. 125–128, September 1966.

[39] W. W. Wierwille and G. A. Gagne, "A theory for the optimal deterministic characterization of the time-varying dynamics of the human operator," NASA CR-170, February 1965.

[40] D. T. McRuer, D. Graham, E. S. Krendel, and W. C. Reisener, Jr., "System performance and operator stationarity in manual control systems," presented at the IFAC Meeting, London, 1966.

[41] J. R. Ward, "The dynamics of a human operator in a control system—A study based on the hypothesis of intermittency," Ph.D. dissertation, University of Sydney, Australia, May 1958.

[42] G. A. Bekey, "The human operator as a sampled-data system," *IRE Trans. Human Factors in Electronics,* vol. HFE-3, pp. 43–51, September 1962.

[43] A. R. Bergen, "On the statistical design of linear random sampling systems," *Automatic and Remote Control (Proc. 1st Internat'l Cong. IFAC),* J. F. Coales *et al.,* Eds. Washington, D. C.: Butterworth, 1961, pp. 430–436.

[44] M. J. Merritt, "An asynchronous pulse-amplitude pulse-width model of the human operator," University of Southern California, School of Elec. Engrg., Rept. 128 August 1966.

[45] R. J. Wasicko, D. T. McRuer, and R. E. Magdaleno, "Human pilot dynamic response in single-loop systems with compensatory and pursuit displays," AFFDL-TR-66-137, December 1966.

[46] R. C. A'Harrah and R. F. Siewert, "Pilot-induced instability," presented at AGARD Specialists Meeting on Stability and Control, Cambridge, England, September 1966.

[47] I. L. Ashkenas, H. R. Jex, and D. T. McRuer, "Pilot-induced oscillations: their cause and analysis," Systems Technology, Inc., TR-239-3 (Northrop-Norair Rept. NOR 64-143), June 1964.

[48] T. S. Durand and G. L. Teper, "An analysis of terminal flight path control in carrier landings," Systems Technology, Inc., TR-137-1, August 1964.

[49] D. G. Ellson and F. E. Gray, "Frequency responses of human operators following a sine-wave input," Air Material Command Memo. Rept. MCREXD-694-2N, December 1948.

[50] C. R. Walston and C. E. Warren, "A mathematical analysis of the human operator in a closed-loop control system," AFPTRC-TR-54-96, 1954.

[51] L. Stark, M. Iida, and P. A. Willis, "Dynamic characteristics of the motor coordination system in man," *Biophysical J.,* vol. 1, 1961.

[52] G. Vossius, "Der Kybernetische Aspekt der Willkurbewegung," *Progress in Cybernetics.* New York: Elsevier, 1965.

[53] F. A. Muckler, R. O. Hookway, and H. H. Burke, "Manned control of large space boosters," *Trans. 7th Symp. Ballistic Missile and Space Technology,* vol. 2, pp. 149–188, August 1962.

[54] R. W. Pew, J. C. Duffendack, and L. K. Fensch, "Sine-wave tracking revisited," 2nd Ann. NASA-University Conf. on Manual Control, NASA SP-128, 1966.

[55] R. A. Hess, "The human operator as an element in a control system with time-varying dynamics," AFFDL-FDCC-TM-65-34, June 1965.

[56] ——, "An investigation of the human operator as an element in both time-variant and equivalent time-invariant systems," AFFDL-FDCC-TM-65-42, September 1965.

[57] E. S. Krendel and D. T. McRuer, "A servomechanisms approach to skill development," *J. Franklin Inst.,* pp. 24–42, January 1960.

[58] D. T. McRuer, I. L. Ashkenas, and H. R. Pass, "Analysis of multiloop vehicular control systems," ASD-TDR-62-1014, March 1964.

[59] R. L. Stapleford, D. T. McRuer, and R. Magdaleno, "Pilot describing function measurements in a multiloop task," NASA CR-542, August 1966.

[60] C. H. Cromwell and I. L. Ashkenas, "A systems analysis of longitudinal piloted control in carrier approach," Systems Technology, Inc., TR-124-1, June 1962.

[61] R. L. Stapleford, J. Wolkovitch, *et al.,* "An analytical study of V/STOL handling qualities in hover and transition," AFFDL-TR-65-73, May 1965.

[62] R. L. Stapleford, D. E. Johnston, *et al.,* "Development of satisfactory lateral-directional handling qualities in the landing approach," NASA CR-239, July 1965.

[63] G. E. Cooper, "Understanding and interpreting pilot opinion," IAS Preprint 683, January 1957.

[64] I. L. Ashkenas and D. T. McRuer, "A theory of handling qualities derived from pilot-vehicle system considerations," Aerospace Engineering, pp. 60, 61, 83–102, February 1962.

[65] H. R. Jex and C. H. Cromwell, "Theoretical and experimental investigation of some new longitudinal handling quality parameters," ASD-TR-61-26, March 1961.

[66] R. P. Harper, Jr., "In-flight simulation of the lateral-directional handling qualities of entry vehicles," WADC-TR-61-147, November 1961.

[67] I. A. M. Hall, "Effects of controlled element on the human pilot," WADC-TR-57-509, August 1958.

[68] I. L. Ashkenas, "A study of conventional airplane handling qualities requirements—I: Roll handling qualities," AFFDL-TR-65-138-I, October 1965.

[69] V. A. Dander, "Predicting pilot ratings of multi-axis control tasks from single-axis data," *IEEE Trans. Human Factors in Electronics,* vol. HFE-4, pp. 15–17, September 1963.